

Dissipative light masks for atomic nanofabrication

**Ralf Stützle §, Dirk Jürgens, Anja Habenicht and
Markus K Oberthaler**

Fachbereich Physik and Optik-Zentrum, Universität Konstanz, D-78457 Konstanz,
Germany

Abstract. We investigate the applicability of laser cooling in intense blue detuned standing light waves for generating nanostructures by direct deposition of atoms on a surface. We report on our results concerning structure width and modulation depth of the resulting structures which are important parameters for future technological applications. As the main result we find that these new masks can lead to a significant reduction of the background. The results have been obtained employing a Monte Carlo simulation which was used to check closed formulas for structure width and background. These results allow a straight forward optimization of the performance of masks for specific experimental parameters and atomic species.

PACS numbers: 32.80Pj, 42.50Vk

Submitted to: *J. Opt. B: Quantum Semiclass. Opt.*

§ To whom correspondence should be addressed (ralf.stuetzle@uni-konstanz.de)

1. Introduction

Atomic nanofabrication, a technique of direct deposition of neutral atoms using conservative far off resonance atom-light interactions has been intensively studied in recent years. Direct deposition has already been demonstrated for sodium [1], chromium [2] and aluminum [3] while experiments with gallium [4], cesium [5], iron [6], and indium are currently under construction. In all these experiments the structures are realized by a sinusoidal conservative potential acting as an array of cylindrical lenses for the atoms. Since the standing light wave acts like a mask, the terminology light masks has been introduced.

The focusing method is very robust and relatively easy to implement experimentally but it has two main drawbacks: the critical dependence of the achievable structure widths on the atomic beam divergence [7] and the non vanishing background also called pedestal. The latter usually does not allow to use the produced structures for technical applications.

Here we present a new concept for light masks in atomic nanofabrication. Combining the traditional focusing methods with the also well known concepts of laser cooling should offer new possibilities in atomic nanofabrication. We will discuss a type of light masks where the atom-light interaction cannot be described with a conservative potential but leads to a damping of the atomic motion during the interaction. This device has no analog in light optics since it focuses like a lense but collimates at the same time. Non-conservative potentials have already been employed in atom lithography using metastable atoms [8]. There the atom-light interaction leads to a spatially modulated loss of atoms and thus allows for the realization of nanostructures using resists. Although the method leads to quantum limited structure widths and negligible pedestal it is only applicable to metastable atoms. In contrast the put forward dissipative light masks can also be employed to ground state atoms.

Since there is a plethora of different cooling schemes [9] we will focus on the most simple cooling process for atoms in a strong blue detuned light wave. This cooling scheme is well understood and has been investigated by a number of authors theoretically [10] as well as experimentally by observing the effect of cooling on the momentum distribution [11][12]. Only few experiments have directly deduced the spatial modulation of the atomic flux inside an intense standing light wave [13].

So far no systematic analyses of the achievable structure widths and pedestals have been performed. In this paper we will utilize a Monte Carlo simulation to verify formulas deduced from simple considerations describing the width and the pedestal of the structures. We find that for a given atomic species the detuning has to be larger than a certain value in order to realize nanostructures with small pedestals. We also observe that the structure width follows a simple scaling formula. Therefore we can estimate the achievable size of the structure features in a simple way.

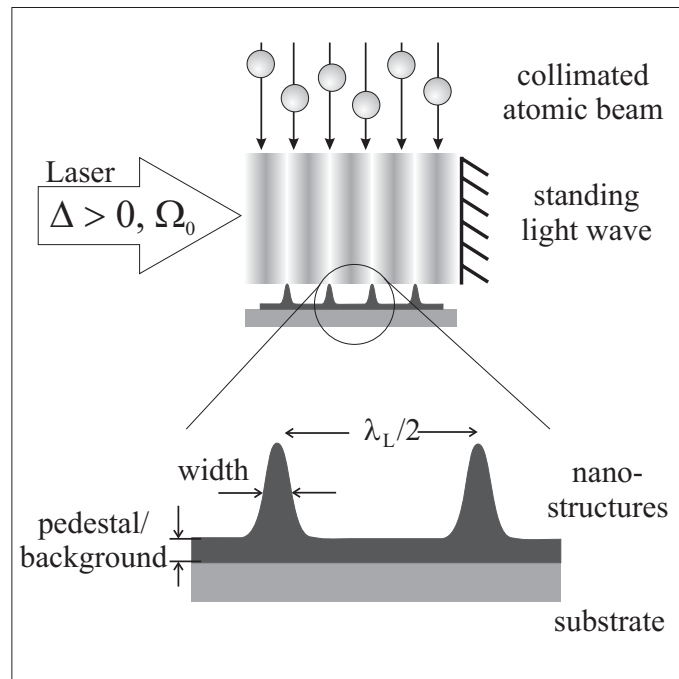


Figure 1. Scheme of an atomic nanofabrication experiment. A collimated beam impinges onto a standing light wave which is realized by retro-reflecting a laser beam from a mirror. The atom-light interaction is characterized by the laser detuning Δ and the Rabi frequency Ω_0 . The feature of the resulting structures are described by the structure width (full width half maximum) and the background also called pedestal. Ideally, the realized nanostructures should have a small width and no pedestal.

2. Physical situation

In this paper we consider the standard situation of an atomic nanofabrication experiment. The flux of a thermal atomic beam is transversally modulated by utilizing light forces (see figure 1) resulting from a standing light wave. As a consequence the deposition rate onto the substrate directly after the atom-light interaction region varies transversally with a period of $\lambda/2$. Thus after some deposition time a thin film with spatially varying thickness is formed on the substrate. This structure is characterized by the width (full width at half maximum) and the pedestal (ratio between background height and maximal height) as indicated in figure 1. Thus in the following we will focus on those two parameters.

We will investigate the transverse atomic flux distribution in a strong standing light wave with frequency higher than the transition frequency (blue detuning). In contrast to the atomic nanofabrication experiments performed so far we analyze the situation where the interaction time $T = 25 \mu\text{s}$ is much larger than the typical time between spontaneous emission events ($1/\Gamma_p \sim 200 \text{ ns}$, where Γ_p is the optical pumping time) and the oscillation time inside the individual potential wells ($T_{os} \sim 250 \text{ ns}$). This is the regime where a Sisyphus type cooling process leads to a narrowing of the initial

momentum distribution [11] but also to a localization of the atoms at the antinodes of the standing light wave [14]. The regime we are interested in is different to the reported channeling regime [13], because spontaneous emission cannot be neglected but is even crucial for the cooling process.

For the following calculations we assume reasonable experimental parameters. As maximal interaction time we have chosen 25 μs which corresponds to a feasible spatial extension of the standing light wave of 2.5 cm for a thermal chromium beam (2000 K, $v_{long} \sim 1000$ m/s). The condition of strong standing light waves implies that the Rabi frequency Ω_0 is much larger than the natural linewidth. In our chromium experiment Rabi frequencies up to 60Γ are feasible. The laser frequency detuning Δ is experimentally adjustable over a wide range and thus can be treated as a free parameter. The intensity distribution of the standing light wave is described by $I(x, z) = I_{max} \sin^2(2\pi x/\lambda)$ where $\lambda = 425$ nm corresponds to the dipole transition ${}^7S_3 \rightarrow {}^7P_4$ in chromium. The Rabi frequency Ω_0 is given by $\Omega_0 = \Gamma \sqrt{I_{max}/2I_s}$ where $\Gamma = 2\pi \times 5$ MHz represents the natural line width of the used transition and $I_s = 8.5$ mW/cm² is the saturation intensity.

Throughout the paper we assume a blue detuned standing light wave i.e. $\Delta > 0$ since for this detuning the cooling naturally leads to a localization of atoms. Theoretical investigations show that a cooling process i.e. a damping force, appears for velocities below a critical velocity v_{cr} whereas faster atoms are even accelerated. This acceleration is a consequence of motionally induced non-adiabatic transitions between different dressed states which become important for fast atoms [15]. The overall performance of the cooling effect can be described by a Sisyphus type process removing kinetic energy which leads to atoms localized in the antinodes of the standing light wave. Since the excitation probability of the atoms near the antinode is minimal the atoms are accumulated in a kind of gray state. This simple picture suggests the formation of a spatially localized atomic distribution.

In the following we will give details of the implemented Monte Carlo simulation [16]. We compare the deduced damping force with the results obtained by integrating the optical Bloch equation utilizing the method of continued fraction [17].

3. Monte Carlo Method

In order to investigate the spatial and momentum distributions of an atomic ensemble inside a strong standing light wave, we employed the very well developed Monte Carlo simulation technique in the dressed state basis [14] [16].

The internal state of the atom in the standing light field is described in the dressed state picture using the local eigenstates corresponding to the transverse position x . With the spatially periodic effective Rabi frequency $\Omega \equiv \Omega(x) = \sqrt{(\Omega_0^2 \sin^2(kx) + \Delta^2)}$ the dressed states are given by

$$|1, n\rangle = \cos \theta |e, n\rangle + \sin \theta |g, n+1\rangle \quad (1)$$

$$|2, n\rangle = -\sin \theta |e, n\rangle + \cos \theta |g, n+1\rangle \quad (2)$$

where θ is defined by

$$\cos(2\theta) = -\frac{\Delta}{\Omega}, \quad \sin(2\theta) = \frac{\Omega_0 \sin(kx)}{\Omega}. \quad (3)$$

The corresponding eigenenergies are given by $E_{1,2} = -\frac{\hbar}{2}(\Delta \pm \Omega)$.

The propagation inside the field leads to a nontrivial coupling between the internal and external degrees of freedom. On the one hand the dressed states can be changed due to spontaneous emission but also due to motionally induced non-adiabatic transitions.

In the following we will lay out how the coupling between the internal and external degrees of freedom is described. The density-matrix equation for the internal degree of freedom in the dressed-state basis (spontaneous emission neglected) for an atom moving with velocity v is given by [16]

$$\begin{aligned} \frac{d\rho_{11}}{dt} &= v \nabla \theta 2\text{Re}(\rho_{12}) \\ \frac{d\rho_{12}}{dt} &= -i\Omega\rho_{12} + v\nabla\theta(1 - 2\rho_{11}), \end{aligned} \quad (4)$$

with

$$\nabla\theta = -\frac{k\Omega_0\Delta \cos(kx)}{2\Omega^2} \quad (5)$$

and the density matrix elements $\rho_{11} = \langle 1, n | \rho | 1, n \rangle$ and $\rho_{12} = \langle 1, n | \rho | 2, n \rangle$.

The position and the velocity of the atom is treated classically and follows Newton's equation of motion $m\dot{v} = f(x)$ where $f(x)$ is a force resulting from averaging over the light fields and internal states. The position x corresponds to the expectation value of x . This force is given by [10]

$$f(x) = -\langle \nabla V(\langle x \rangle) \rangle = \frac{\hbar \nabla \Omega}{2} (1 - 2\rho_{11}) - 2\hbar \Omega \text{Re}(\rho_{12}) \nabla \theta \quad (6)$$

with

$$\nabla \Omega = \frac{k \Omega_0^2 \sin(2kx)}{2\Omega}. \quad (7)$$

The Monte Carlo method allows to implement the diffusive character of the interaction in a straightforward and simple way by modelling the spontaneous emissions as a stochastic process during the integration. For the final result one has to average over many realizations (typically 4000 trajectories). Between the spontaneous emission events the density-matrix elements evolve according to the set of differential equations (4) and the atomic motion is given by solving Newton's equation of motion with the instantaneous force given by equation (6). This evolution is implemented using a Runge-Kutta integration procedure of 4th order for a typical time step of $\delta t \sim 1$ ns. After this integration time the spontaneous emission probability for the evolved superposition state $|\Psi\rangle = c_1|1, n\rangle + c_2|2, n\rangle$ is given by

$$p_s = \Gamma \left(\rho_{11} \cos^2 \theta - 2\text{Re}(\rho_{12}) \cos \theta \sin \theta + (1 - \rho_{11}) \sin^2 \theta \right) \delta t. \quad (8)$$

The branching ratio between the decay from $|\Psi\rangle$ to $|1, n-1\rangle$ and the decay to $|2, n-1\rangle$ respectively is given by

$$\eta = \frac{\sin^2 \theta}{\cos^2 \theta}. \quad (9)$$

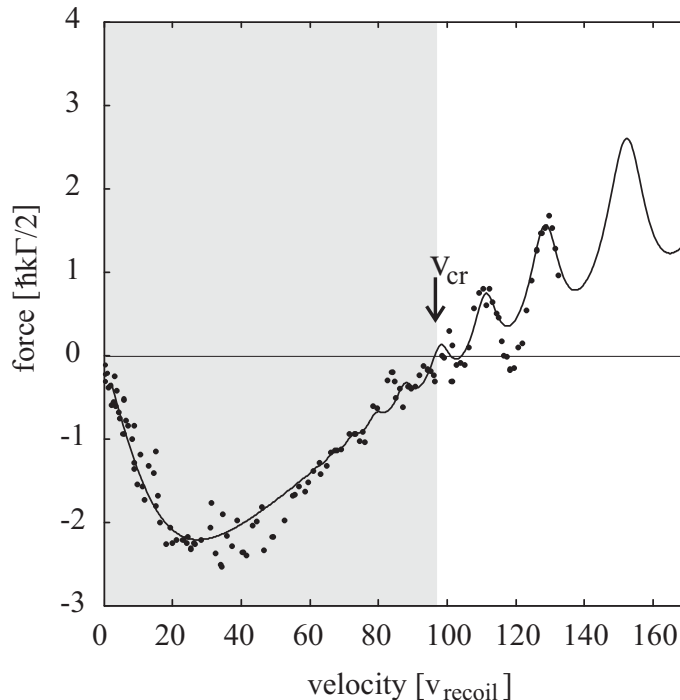


Figure 2. Velocity dependence of the spatially averaged light force in a strong standing light wave for lithium atoms ($\Omega_0 = 50\Gamma$, $\Delta = 15\Gamma$). The solid line represents the result obtained by solving the optical Bloch equations using the continued fraction method. The points are the result of the implemented Monte Carlo simulation. Both methods agree reasonably well. A very important feature is that the force is only decelerating below a critical velocity v_{cr} (indicated by the gray shading).

For each integration step two pseudorandom numbers homogeneously distributed over the interval $[0, 1]$ are chosen. The first number is compared to the transition probability p_s given by equation (8) and determines whether a spontaneous emission event has occurred. The second random number compared with η given by equation (9) governs onto which state the atom is projected as an initial condition for further propagation. For our parameter set the effect of the recoil kick due to the spontaneously emitted photon is small compared to the acceleration resulting from the potential change when the dressed state is altered. Therefore it has been neglected. After many independent simulations the expected spatial and momentum distribution can be deduced by averaging over the calculated trajectories.

In order to check the reliability of the results obtained from our simulation we deduce the time and spatially averaged force on an atom as a function of the initial velocity from the trajectories. These results can be directly compared to the force obtained by the continued fraction method [17]. For the graph in figure 2 we assume lithium atoms in a standing light wave ($\Omega_0 = 50\Gamma$, $\Delta = 15\Gamma$) such that our results can be directly compared with the results in [16]. Figure 2 reveals that the two independent calculations agree reasonably. Especially the critical velocity is reproduced quite well by the Monte Carlo method. Since the force is deduced by analyzing averaged trajectories

care has to be taken by choosing the averaging time. This is especially critical at the Doppleron resonances [18][19] where a constant velocity change in time i.e. constant force, is only true for short interaction times.

An important parameter for the following discussion is the critical velocity v_{cr} which specifies where the averaged force changes from a decelerating to an accelerating force. Thus atoms faster than v_{cr} will not be cooled but are even accelerated to higher velocities. This change of the characteristics of the force results from non-adiabatic transitions between dressed states.

4. Results of simulations

In the following we will discuss in detail the obtained results addressing the questions of achievable widths of the nanostructures and the pedestal. Specifically we have chosen the system of chromium atoms in a standing light wave near resonant with the optical transition ${}^7S_3 \rightarrow {}^7P_4$. For the simulations a perfectly collimated incident atomic beam was assumed. This is no limitation with respect to applicability of our results to real experiments with a finite velocity distribution because the periodic dipole force anyway accelerates the atoms immediately to a maximum velocity $v_{max} \sim \sqrt{\hbar\Omega_0/m}$. This is on the order of few m/s. Thus an atomic beam transversally Doppler cooled is well described by our theory. Our simulations for one longitudinal velocity show that the resulting structures do not depend critically on the interaction time (figure 3). Therefore the predictions presented in this work are directly applicable to a thermal beam. This insensitivity to the initial preparation of the atomic beam is one of the strengths of the dissipative light masks.

In figure 3 we summarize the results concerning the pedestal of the nanostructures for a very diverse parameter set of Rabi frequencies Ω_0 , detunings Δ and an interaction time of $25 \mu\text{s}$. The filled circles represent the parameter sets where the pedestal is smaller than 15% while the open circles account for structures with a background larger than 15%. Clearly the background gets worse for smaller detunings which can be understood on the basis of the critical velocity. The boundary line drawn in figure 3 between the two regimes is defined as $v_{cr} = \overline{v_{max}} = 1.6 \text{ m/s}$ where v_{cr} has been obtained by solving the optical Bloch equations. The velocity $\overline{v_{max}} = 1.6 \text{ m/s}$ is an approximate value of v_{max} accounting for the velocity spread due to the dipole force fluctuations [10][16]. Hence this is not a strict boundary but gives a hint for which parameters the background starts to become significant.

The pedestal can be attributed to the initial acceleration of the atoms in the conservative part of the periodic potential of the standing light wave. If the atom is accelerated beyond the critical velocity v_{cr} , no damping force will act on the particle anymore. Thus those atoms are further accelerated and show up as background. This dependence is directly revealed in the velocity distribution of the pedestal, which can be deduced from the data obtained from the simulation. In figure 4 the results for $\Omega_0 = 80\Gamma$ and $\Delta = 16\Gamma$ and $\Delta = 10\Gamma$ respectively are shown. Clearly the graphs exhibit that for

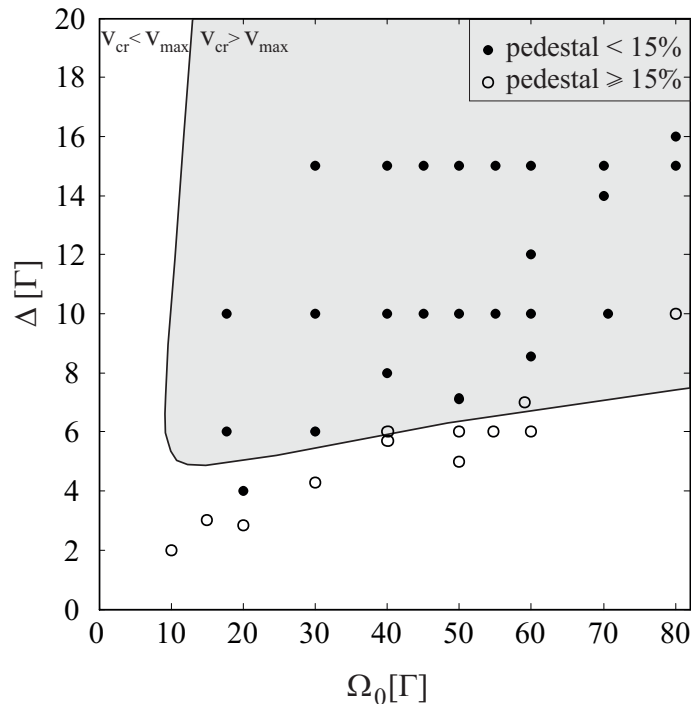


Figure 3. Results on the pedestal for chromium nanostructures for an interaction time of $25 \mu\text{s}$ as a function of the Rabi frequency Ω_0 , detuning Δ . Filled/open circles represent structures with a pedestal smaller/bigger than 15%. The solid line separating the two regions indicates where the condition $v_{cr} = v_{max} = 1.6 \text{ m/s}$ is fulfilled. This line has to be understood as a smooth boundary due to the fluctuation of the dipole force, but it shows that there is a minimal detuning for which structures with small pedestals are attainable.

the latter case the background atoms are accelerated up to 10 m/s and thus cannot be cooled into the dipole potential minima. It is important to note that in this case the number of atoms in the pedestal is not reduced but even increases slightly for longer interaction times (see lower right graph in figure 4). This is a result of the dipole force fluctuations and the small v_{cr} for the chosen parameters. In the case of $v_{max} < v_{cr}$ the background slowly diminishes which is a consequence of the cooling process damping the motion of the atoms. The main result with respect to background is that the detuning has to be chosen larger than a certain critical value which is $\Delta_{cr} = 6\Gamma$ for chromium. In section 5 we report on Δ_{cr} we have obtained for other elements. The absolute value of the background can be reduced by increasing detuning and Rabi frequency at the same time. Thus we find the minimal background of 7.3% for parameters $\Omega_0 = 80\Gamma$ and $\Delta = 16\Gamma$. This cannot be directly compared to the 'ultimate' values of pedestal 14% for standard focussing techniques given in [20] because this value is critically dependent on the incident beam divergence. In the case of dissipative light masks the given value is also true for a divergent beam as long as the maximal transverse velocity is smaller than v_{cr} which is in the order of few m/s.

Another very important characteristic of the dissipative light masks is the achievable

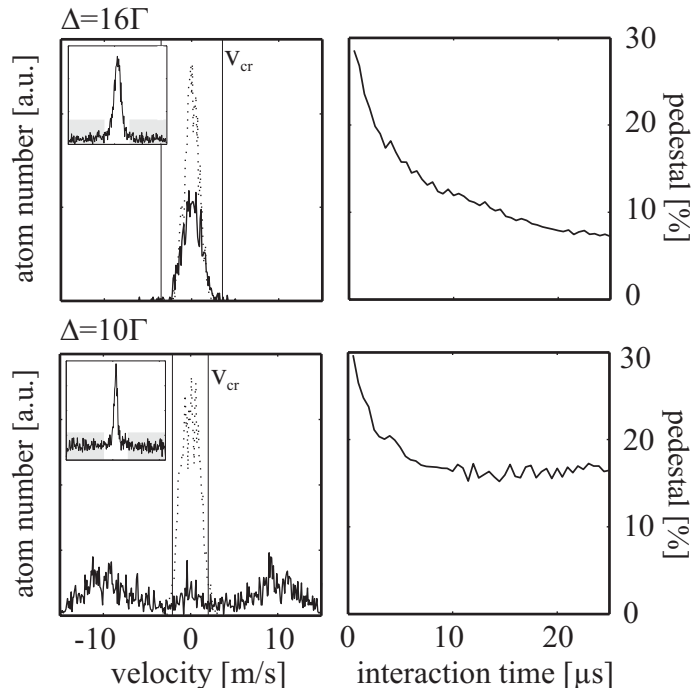


Figure 4. Velocity distribution (left row) and number of atoms in the pedestal as a function of interaction time (right row) for $\Omega_0 = 80\Gamma$ and the indicated detuning Δ . The dotted/solid lines represent the velocity distribution of the pedestal as indicated in the insert (spatial distribution after 25 μ s) after 500 ns/25 μ s. This makes clear that the background for small detunings is a consequence of the initial acceleration of atoms to a velocity larger than the critical velocity. Important to note is that the pedestal reduces in time if all atoms are slower than the critical velocity while in the other case the background even starts to grow for longer times.

structure width. Figure 4 reveals that smaller structure features can be expected for smaller detuning. Thus it seems that either the parameters are chosen for minimal pedestal or for small features. In the following we will show that a closed formula can be deduced for the width of the nanostructures which allows to optimize the parameters for the combination of minimal structures and suppressed background.

It has already been mentioned that the cooling in strong standing light waves has the characteristics of Sisyphus cooling into a gray state. An estimate of the gray state's spatial size i.e. structure width, is straight forward. The potential at its minimum is harmonic with the oscillation frequency ω_{os} given by

$$\omega_{os} = \Omega_0 \sqrt{\frac{\omega_{rec}}{\Delta}} \quad (10)$$

where $\omega_{rec} = \hbar k^2/2m$ represents the recoil frequency. This harmonic potential is a trapping potential for atoms in the dressed state $|1, n\rangle$ while it is an expulsive potential for atoms in the dressed state $|2, n\rangle$. In order to estimate the decay out of the localized state we calculate the mean decay rate $\bar{\Gamma}_{1 \rightarrow 2}$ by averaging the local decay rate $\Gamma_{1 \rightarrow 2}(x) = \Gamma \cos^4 \theta(x)$ over the harmonic motion $x(t) = x_0 \sin(\omega_{os} t)$. If nanostructures should be formed, this decay has to be balanced by a filling rate due to the cooling force.

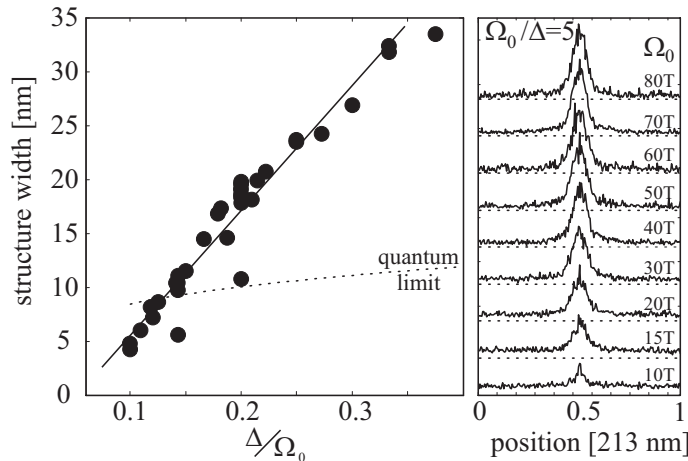


Figure 5. Scaling law for the structure width. The results on structure width are plotted as a function of the scaling parameter Δ/Ω_0 . The graph reveals that the scaling law is fulfilled. The straight line is a guide to the eye. The quantum limit is given by the size of the lowest bound state in the periodic potential. The right hand side graph shows the atomic distribution after $25 \mu\text{s}$ for different Rabi frequencies while the detuning was adjusted according to $\Delta = \Omega_0/5$.

We therefore introduce a characteristic time τ and equate $1/\tau$ and the decay rate $\bar{\Gamma}_{1 \rightarrow 2}$. As a result we find for the expected maximal oscillation amplitude x_0 of the localized atoms

$$x_0 = \frac{\Delta}{k\Omega_0} \sqrt[4]{\frac{128}{3\Gamma} \frac{1}{\tau}}. \quad (11)$$

Hence we expect a scaling of the structure width with Δ/Ω_0 . The absolute value of the structures can be evaluated knowing the parameter τ which we have deduced from Monte Carlo simulations for different atomic species given in section 5.

In figure 5 the structure width for all used parameter sets are plotted as a function of the scaling parameter Δ/Ω_0 . It clearly reveals the expected linear dependence and thus allows to simply estimate the structure width for given parameters. It is important to note that the calculation does not include the quantum nature of the particle motion. Therefore we have included in figure 5 the quantum limit showing the ground state size (full width at half maximum) for the chosen parameters revealing the limit of applicability of the used semiclassical theory. A very different question is how much the growth process and surface diffusion determines the final width of the nanostructures and is still an open question [21].

In figure 5 also structures for different laser intensities are shown i.e. different Ω_0 but the detuning was chosen to fulfill the condition $\Omega_0 = 5\Delta$. Clearly the width does not change while the background diminishes for increasing intensity.

Element (transition)	τ [μ s]	Δ_{cr} [Γ]	$\Omega_{15\text{nm}}$ [Γ]
Cr (425 nm)	4.6	6.0	46
Fe (372 nm)	10.0	9.5	63
Ga (294 nm)	3.0	3.4	15
Cs (852 nm)	1.2	2.4	44

Table 1. Dissipative light mask parameters for different elements. The focusing parameter τ as defined in (equation 11) is obtained by Monte Carlo simulations while the minimal detuning Δ_{cr} for a reduced background follows from the solution of the Bloch equation using the continued fraction method. The Rabi frequency given in the fourth column leads with $\Delta = \Delta_{cr}$ to a structure width of 15 nm (equation 11).

5. Optimal parameters for dissipative light masks

Our simulations show that dissipative light masks are very versatile. Analyzing the parameter space we find that the background can be significantly reduced (<15%) for structure widths down to 15 nm. For chromium we find that the critical detuning of $\Delta_{cr} = 6\Gamma$ leads to the smallest structures with minimal background. These results suggest that with the currently existing experimental setup (laser power of 500 mW and interaction time of 25 μ s) we can expect 15 nm lines with a background of 10% for standing light wave parameters $\Omega_0 = 30\Gamma$ and $\Delta = 6\Gamma$.

It is important to note that our results are also applicable to other atomic species with a closed transition $F \rightarrow F + 1$ such that a two level system can be experimentally realized by optical pumping. The structure width for different elements can be predicted, if the free parameter τ in equation (11) is given. In order to work in the cooling regime leading to a reduced background the detuning of the standing light wave has to be chosen larger than a critical value Δ_{cr} which is also element specific. Our results for different atomic species are summarized in table 1.

6. Conclusion

In this paper we discussed the basic features of dissipative light masks realized by intense blue detuned standing light waves. We analyzed the important parameters such as structure width and pedestal. We find that for a given atomic species an optimal parameter set for both, minimal structure width and background, exists. We also give optimal values for different elements. These new types of masks also allow to tune in a well defined way the structure width given by a simple scaling law of experimentally directly controllable parameters.

Acknowledgments

We thank Jürgen Mlynek for encouragement and support. This research is funded by the SFB513 of the Deutsche Forschungsgemeinschaft and by the RTN network

”Cold quantum gases” under Contract No. HPRN-CT-2000-00125. M. O. especially acknowledges an Emmy Noether fellowship from the Deutsche Forschungsgemeinschaft.

References

- [1] Timp G, Behringer R E, Tennant D M, Cunningham J E, Prentiss M and Bergren K K 1992 *Phys. Rev. Lett.* **69** 1636
- [2] McClelland J J, Scholten R E, Palm E C and Celotta R J 1993 *Science* **262** 877
Drozdofsky U, Stuhler J, Brezger B, Schulze T, Drewsen M, Pfau T and Mlynek J 1997 *Microelectronic Engineering* **35** 285
Sun H B, Inouye H, Inouye Y, Okamoto K and Kawata S 2001 *Jpn. J. Appl. Phys.* **40** L711
Jurdik E, Hohlfeld J, van Kempen H, Rasing Th and McClelland J J 2002 *Appl. Phys. Lett.* **80** 4443
- [3] McGowan R W, Giltner D M and Lee S A 1995 *Opt. Lett.* **20** 2535
- [4] Rehse S J, Fairbank W M Jr and Lee S A 2001 *J. Opt. Soc. Am. B* **18** 855
- [5] Camposo A, Piombini A, Cervelli F, Tantussi F, Fuso F and Arimondo E 2001 *Opt. Commun.* **200** 231
- [6] te Sligte E, Bosch R C M, Smeets B, van der Straten P, Beijerinck H C W and van Leeuwen K A H 2002 *Proc. Natl. Acad. Sci.* **99** 6509
- [7] McClelland J J 1995 *J. Opt. Soc. Am. B* **12** 1761
- [8] Johnson K S, Thywissen J H, Dekker N H, Berggren K K, Chu A P, Younkin R and Prentiss M 1998 *Science* **280** 1583
- [9] Metcalf J and van der Straten P 1999 *Laser Cooling and Trapping* (Springer-Verlag, New York)
- [10] Dalibard J and Cohen-Tannoudji C 1985 *J. Opt. Soc. Am. B* **2** 1707
- [11] Aspect A, Dalibard J, Heidmann A, Salomon C and Cohen-Tannoudji C 1986 *Phys. Rev. Lett.* **57** 1688
- [12] Chen J, Story J G, Tollett J J and Hulet R G 1992 *Phys. Rev. Lett.* **69** 1344
- [13] Salomon C, Dalibard J, Aspect A, Metcalf H and Cohen-Tannoudji C 1987 *Phys. Rev. Lett.* **59** 1659
- [14] Dalibard J, Heidmann A, Salomon C, Aspect A, Metcalf H and Cohen-Tannoudji C 1989 *Fundamentals of Quantum Optics II*, edited by Ehlötzky F (Springer-Verlag, Berlin) p 196
- [15] Mølmer K 1992 *Phys. Scr.* **45** 246
- [16] Chen J, Story J G and Hulet R G 1993 *Phys. Rev. A* **47** 2128
- [17] Minogin V G and Serimaa O T 1979 *Opt. Commun.* **30** 373
- [18] Kyrölä E and Stenholm S 1977 *Opt. Commun.* **22** 123
- [19] Bigelow N P and Prentiss M G 1990 *Phys. Rev. Lett.* **65** 555
Tollett J J, Chen J J, Story J G, Ritchie N W M, Bradley C C and Hulet R G 1990 *Phys. Rev. Lett.* **65** 559
- [20] Jurdik E, Rasing T, van Kempen H, Bradley C C and McClelland J J 1999 *Phys. Rev. B* **60** 1543
- [21] Anderson W R, Bradley C C, McClelland J J and Celotta R J 1999 *Phys. Rev. A* **59** 2476